World Academy of Science, Engineering and Technology
International Journal of Mathematical and Computational Sciences
Vol:18, No:7, 2024

Labyrinth Fractal on a Convex Quadrilateral

Harsha Gopalakrishnan, Srijanani Anurag Prasad

Abstract—Quadrilateral Labyrinth Fractals are a type of fractals presented in this paper. They belong to a unique class of fractals on any plane quadrilateral. The previously researched labyrinth fractals on the unit square and triangle inspire this form of fractal. This work describes how to construct a quadrilateral labyrinth fractal and looks at the circumstances in which it can be understood as the attractor of an iterated function system. Furthermore, some of its topological properties and the Hausdorff and box-counting dimensions of the quadrilateral labyrinth fractals are studied.

Keywords—Fractals, labyrinth fractals, dendrites, iterated function system, non-self similar, non-self affine, connected, path connected.

I. Introduction

LABYRINTH fractals are a type of Sierpinski carpet in the plane. Cristea and Steinsky [1], [2] introduced labyrinth fractals on a unit square in a plane. In the same work, they also explored Hausdorff dimensions and a few topological properties. Labyrinth sets that meet tree, exit, and corner parameters are the building blocks for labyrinth fractals. Triangular labyrinth fractals are a related idea that Cristea and Paul Surer [3] introduced, wherein two triangle pattern systems form the foundation for fractal construction. As a result, two fractals are produced. Labyrinth fractals are self-similar dendrites in both square and triangular cases. The ideas around labyrinth fractals on the unit square were expanded upon in several ways, including creating mixed and super-mixed labyrinth fractals [4], [5]. A series of labyrinth patterns are used to create mixed labyrinth fractals. i.e., different patterns are used at various iteration phases. Super-mixed labyrinth fractals employ a finite array of patterns at every iteration step. Labyrinth fractals that are mixed or super-mixed typically aren't self-similar.

Introduced by Cristea and Stiensky, the classical labyrinth fractal on a square has many uses in physics, including the fractal reconstruction of complex images, signals, and radar backgrounds [6], planar nanostructures [7], and the construction of prototypes of ultra-wide-band radar antennas [8]. In telecommunication, fractal labyrinths and genetic algorithms are coupled to synthesise large, resilient antenna arrays and nanoantennas [9].

The labyrinth fractal can be extended to any convex quadrilateral in a plane. Quadrilaterals do not exhibit self-similarity when split into smaller quadrilaterals, in contrast to the creation of labyrinth fractals in squares and triangles. Therefore, self-similarity cannot exist in this class of fractals. As a result, it is fascinating to investigate the labyrinth fractal on a convex quadrilateral, which has the same qualities as the square and triangle cases but lacks similarity at each stage of development.

Harsha Gopalakrishnan and S.A. Prasad are with the Department of Mathematics and Statistics at Indian Institute of Technology Tirupati, India (e-mail: harshagopal3@gmail.com, srijanani@iittp.ac.in).

The first task in the paper is to build a fractal on a convex quadrilateral in Section II. Instead of similar quadrilaterals, the produced set is a set of similar quadrilaterals with two types of parallelograms at each stage of construction. This section also includes some preliminary results. This study defines labyrinth fractals on convex quadrilaterals and discusses their fundamental characteristics in Section III. The concept aligns precisely with the earlier definitions for triangles and squares, i.e., the quadrilateral labyrinth satisfies the corner, exit, and tree properties. Specific requirements on quadrilaterals are derived in Section IV so that the maps that generate the quadrilateral labyrinth fractal form an iterated function system. The box-counting dimension of quadrilateral labyrinth fractals is covered in Section V. The fundamental definition is used to find the dimension. The Hausdorff dimension of the quadrilateral labyrinth fractals is provided in Section VI. In Section VII, the topological features are discussed. In addition to the topological characteristics of the labyrinth fractal itself, the work addresses the topological qualities of complements of labyrinths on the quadrilaterals, which was not studied in the case of squares and triangles.

When self-similarity is absent, the labyrinth fractal in the convex quadrilateral can be used. In any real-life setting, the basic framework of the research does not have to be square or triangle-shaped. The labyrinth fractal on the quadrilateral can be employed in this scenario because it works with any four-sided convex polygon in a plane.

II. Construction of Fractal

This section describes the construction of a fractal on any convex quadrilateral on a plane. A few initial construction-related outcomes are also demonstrated. These findings will aid in the proof of different theorems in subsequent sections.

On a plane, let Q be a convex quadrilateral. Using the quadrilateral's smallest diagonal (or any of them if they are equal diagonals), the quadrilateral is divided into two triangles. This diagonal is referred to as the common side for the resulting triangles. For the triangles that result, the common points are the ends of the common side. The quadrilateral is designated as follows: Moving anticlockwise, the vertices of Q are denoted as Q_1, Q_2, Q_3, and Q_4, respectively, starting from any of the common points (see Fig. 1). So, $\Delta_1 = Q_1Q_2Q_3$ and $\Delta_2 = Q_3Q_4Q_1$ are the triangles that result from the quadrilateral $Q = Q_1Q_2Q_3Q_4$.

If $x \in Q$ then $x \in \Delta_1$ or $x \in \Delta_2$. Suppose $x \in \Delta_1$. Then $x = \alpha_1Q_1 + \alpha_2Q_2 + \alpha_3Q_3$ is the unique representation in Δ_1, with $\alpha_1 + \alpha_2 + \alpha_3 = 1$ and $\alpha_1, \alpha_2, \alpha_3 \geq 0$. So, $x = \alpha_1Q_1 + \alpha_2Q_2 + \alpha_3Q_3 + 0Q_4$ uniquely represents the point x in Q. Similarly, suppose $x \in \Delta_2$. Then $x = \alpha_3Q_3 + \alpha_4Q_4 +$

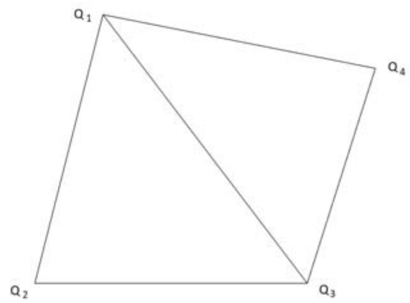

Fig. 1 An example of the naming of a quadrilateral

$\alpha_1 Q_1$ is the unique representation in Δ_2, with $\alpha_3 + \alpha_4 + \alpha_1 = 1$ and $\alpha_3, \alpha_4, \alpha_1 \geq 0$. So, $x = \alpha_1 Q_1 + 0Q_2 + \alpha_3 Q_3 + \alpha_4 Q_4$ gives a unique representation of x in Q. The definitions above coincide when x lies on the line Q_1Q_3. Since α_i is the coefficient of Q_i, each $x \in Q$ can be uniquely represented as $(\alpha_1, \alpha_2, \alpha_3, \alpha_4)$, where $i = 1, 2, 3, 4$, as in the previous representation, with either $\alpha_2 = 0$ or $\alpha_4 = 0$.

Definition 1: Let $Q = Q_1Q_2Q_3Q_4$ and $R = R_1R_2R_3R_4$ be two convex quadrilaterals. Define the map $P_R : Q \to R$ as $P_R(x) = \alpha_1 R_1 + \alpha_2 R_2 + \alpha_3 R_3 + \alpha_4 R_4$, where $(\alpha_1, \alpha_2, \alpha_3, \alpha_4)$ is the unique representation of x in Q.

Let X and Y be two topological spaces. A homeomorphism from X to Y is a bijection $f : X \to Y$ such that both f and f^{-1} are continuous.

Proposition 1: Let $R = R_1R_2R_3R_4$ be a convex quadrilateral inside a convex quadrilateral $Q = Q_1Q_2Q_3Q_4$. When $(\alpha_1, \alpha_2, \alpha_3, \alpha_4)$ is the unique representation of x in Q, then the map $P_R : Q \to R$ given by $P_R(x) = \alpha_1 R_1 + \alpha_2 R_2 + \alpha_3 R_3 + \alpha_4 R_4$ is a homeomorphism between Q and R.

Proof: Let $P_R(x) = P_R(y)$ for $x, y \in Q$ with $(\alpha_1, \alpha_2, \alpha_3, \alpha_4)$ and $(\beta_1, \beta_2, \beta_3, \beta_4)$ as the unique representation of x and y in Q respectively.

Case 1: $x \in \Delta_1 = Q_1Q_2Q_3$ and $y \in \Delta_2 = Q_1Q_3Q_4$.

In this case, $x = (\alpha_1, \alpha_2, \alpha_3, 0)$ and $y = (\beta_1, 0, \beta_3, \beta_4)$ in Q. So $P_R(x) = P_R(y)$ in R gives $(\alpha_1, \alpha_2, \alpha_3, 0) = (\beta_1, 0, \beta_3, \beta_4)$. Thus $\alpha_1 = \beta_1$, $\alpha_2 = 0$, $\alpha_3 = \beta_3$, $\beta_4 = 0$ and so $x = y$ and lies on the line joining Q_1 and Q_3.

Case 2: $x, y \in \Delta_1 = Q_1Q_2Q_3$ or $x, y \in \Delta_2 = Q_3Q_4Q_1$

In this case, $x = (\alpha_1, \alpha_2, \alpha_3, 0)$ and $y = (\beta_1, \beta_2, \beta_3, 0)$ or $x = (\alpha_1, 0, \alpha_3, \alpha_4)$ and $y = (\beta_1, 0, \beta_3, \beta_4)$ in Q. So $P_R(x) = P_R(y)$ in R gives $(\alpha_1, \alpha_2, \alpha_3, 0) = (\beta_1, \beta_2, \beta_3, 0)$ or $(\alpha_1, 0, \alpha_3, \alpha_4) = (\beta_1, 0, \beta_3, \beta_4)$. In either case $\alpha_i = \beta_i$ for $i = 1, 2, 3, 4$ and so $x = y$.

Consequently, P_R is injective. Surjectivity derives from the definition of P_R; hence, P_R is a bijection.

Consider a sequence $(x_n) = \alpha_{1n} Q_1 + \alpha_{2n} Q_2 + \alpha_{3n} Q_3 + \alpha_{4n} Q_4$ in Q that converges to $x = \alpha_1 Q_1 + \alpha_2 Q_2 + \alpha_3 Q_3 + \alpha_4 Q_4$ in Q. Then $(\alpha_{1n}, \alpha_{2n}, \alpha_{3n}, \alpha_{4n})$ is a sequence in $\mathbb{R}^4$ converging to $(\alpha_1, \alpha_2, \alpha_3, \alpha_4)$ in $\mathbb{R}^4$ which gives $(\alpha_{in}) \to \alpha_i$ for $i = 1, 2, 3, 4$. Therefore, $(\alpha_{1n} R_1 + \alpha_{2n} R_2 + \alpha_{3n} R_3 + \alpha_{4n} R_4) \to \alpha_1 R_1 + \alpha_2 R_2 + \alpha_3 R_3 + \alpha_4 R_4$. As a result, P_R is continuous since $P_R(x_n) \to P_R(x)$. Similarly, $(P_R)^{-1}$ is likewise continuous. Consequently, P_R is a homeomorphism. ∎

For $m \geq 2$, consider the sets
$A_1 = \{(k_1, k_2, k_3, k_4) \in (\mathbb{N} \cup \{0\})^4 : k_1 + k_2 + k_3 = m - 1, k_4 = 0 \text{ and } k_2 \neq 0\}$
$A_2 = \{(k_1, k_2, k_3, k_4) \in (\mathbb{N} \cup \{0\})^4 : k_1 + k_3 + k_4 = m - 1, k_2 = 0 \text{ and } k_4 \neq 0\}$
$A_3 = \{(k_1, k_2, k_3, k_4) \in (\mathbb{N} \cup \{0\})^4 : k_1 + k_3 = m - 1 \text{ and } k_2 = k_4 = 0\}$.
Let

$$A = A_1 \cup A_2 \cup A_3 \tag{1}$$

Define a function S_m on A as
$S_m(k_1, k_2, k_3, k_4) = R_1R_2R_3R_4$, where

$$R_1 = \frac{(k_1+1)Q_1 + k_2Q_2 + k_3Q_3 + k_4Q_4}{m},$$
$$R_2 = \frac{k_1Q_1 + (k_2+1)Q_2 + k_3Q_3 + k_4Q_4}{m},$$
$$R_3 = \frac{k_1Q_1 + k_2Q_2 + (k_3+1)Q_3 + k_4Q_4}{m},$$
$$R_4 = \frac{(k_1+1)Q_1 + (k_2-1)Q_2 + (k_3+1)Q_3 + k_4Q_4}{m}$$
if $(k_1, k_2, k_3, k_4) \in A_1$

$$R_1 = \frac{(k_1+1)Q_1 + k_2Q_2 + k_3Q_3 + k_4Q_4}{m},$$
$$R_2 = \frac{(k_1+1)Q_1 + k_2Q_2 + (k_3+1)Q_3 + (k_4-1)Q_4}{m},$$
$$R_3 = \frac{k_1Q_1 + k_2Q_2 + (k_3+1)Q_3 + k_4Q_4}{m},$$
$$R_4 = \frac{k_1Q_1 + k_2Q_2 + k_3Q_3 + (k_4+1)Q_4}{m}$$
if $(k_1, k_2, k_3, k_4) \in A_2$,

$$R_1 = \frac{(k_1+1)Q_1 + k_2Q_2 + k_3Q_3 + k_4Q_4}{m},$$
$$R_2 = \frac{k_1Q_1 + (k_2+1)Q_2 + k_3Q_3 + k_4Q_4}{m},$$
$$R_3 = \frac{k_1Q_1 + k_2Q_2 + (k_3+1)Q_3 + k_4Q_4}{m},$$
$$R_4 = \frac{k_1Q_1 + k_2Q_2 + k_3Q_3 + (k_4+1)Q_4}{m}$$
if $(k_1, k_2, k_3, k_4) \in A_3$.

Then $S_m(k_1, k_2, k_3, k_4)$ are parallelograms in Q for $(k_1, k_2, k_3, k_4) \in A_1 \cup A_2$. For $(k_1, k_2, k_3, k_4) \in A_3$, $S_m(k_1, k_2, k_3, k_4)$ are quadrilaterals in Q which are similar to Q.

Let $\mathcal{S}_m = S_m(A_1) \cup S_m(A_2) \cup S_m(A_3)$. The corner quadrilaterals are the members of the set $C = \{S_m(m-1, 0, 0, 0),\ S_m(0, m-1, 0, 0),\ S_m(0, 0, m-1, 0),\ S_m(0, 0, 0, m-1)\} \subseteq \mathcal{S}_m$. Border quadrilaterals are those elements $S_m(k_1, k_2, k_3, k_4)$ in $\mathcal{S}_m$, which has at most two of the k_i's as nonzero.

Now choose a subset $\mathcal{W}_1$ of $\mathcal{S}_m$, which is called the set of white quadrilaterals of order 1 and $\mathcal{B}_1 = \mathcal{S}_m \setminus \mathcal{W}_1$ is called the set of black quadrilaterals of order 1. For $n \geq 2$, the set of white quadrilaterals of order n is given by $\mathcal{W}_n = \{P_{W_{n-1}}(W_1) : W_1 \in \mathcal{W}_1, W_{n-1} \in \mathcal{W}_{n-1}\}$. Then $\mathcal{W}_n \subset \mathcal{S}_{m^n}$ and the set of black squares of order n is given by $\mathcal{B}_n = \mathcal{S}_{m^n} \setminus \mathcal{W}_n$. For $n \geq 1$, define $L_n = \bigcup_{W \in \mathcal{W}_n} W$. Since each L_n is closed and bounded, L_n is compact. Thus, $\{L_n\}$ is a monotonically decreasing sequence of compact sets. The fractal set in Q is defined as $\mathcal{L}_\infty = \bigcap_{n=1}^{\infty} L_n$.

Proposition 2: Let $Q = Q_1Q_2Q_3Q_4$ be a convex quadrilateral, and $\mathcal{S}_m$ be defined as above for any $m \geq 2$. Then
$P_{Q'} \circ P_{Q''} = P_S$ in Q, where $S = P_{Q'}(Q'')$ and $Q'' \in \mathcal{S}_n$ for any $n \geq m$.

Proof: Let $Q' = R_1R_2R_3R_4$ and $Q'' = T_1T_2T_3T_4$. Suppose $T_i = \alpha_1^i Q_1 + \alpha_2^i Q_2 + \alpha_3^i Q_3 + \alpha_4^i Q_4$ is the unique representation of T_i in Q for $i = 1, 2, 3, 4$. Choose $x \in Q$. WLOG suppose that $x \in \Delta_1$ and let $x = \beta_1 Q_1 + \beta_2 Q_2 + \beta_3 Q_3 + 0Q_4$ be the unique representation of x in Q.

Case 1: Q'' in Δ_1. In this case, $\alpha_4^i = 0$ for all $i = 1, 2, 3, 4$. Then,

$$
\begin{aligned}
P_{Q'} \circ P_{Q''}(x) &= P_{Q'} \circ P_{Q''}(\beta_1 Q_1 + \beta_2 Q_2 + \beta_3 Q_3) \\
&= P_{Q'}(\beta_1 T_1 + \beta_2 T_2 + \beta_3 T_3) \\
&= P_{Q'}(\beta_1(\alpha_1^1 Q_1 + \alpha_2^1 Q_2 + \alpha_3^1 Q_3) \\
&\quad + \beta_2(\alpha_1^2 Q_1 + \alpha_2^2 Q_2 + \alpha_3^2 Q_3) \\
&\quad + \beta_3(\alpha_1^3 Q_1 + \alpha_2^3 Q_2 + \alpha_3^3 Q_3)) \\
&= P_{Q'}((\beta_1\alpha_1^1 + \beta_2\alpha_1^2 + \beta_3\alpha_1^3)Q_1 \\
&\quad + (\beta_1\alpha_2^1 + \beta_2\alpha_2^2 + \beta_3\alpha_2^3)Q_2 \\
&\quad + (\beta_1\alpha_3^1 + \beta_2\alpha_3^2 + \beta_3\alpha_3^3)Q_3) \\
&= (\beta_1\alpha_1^1 + \beta_2\alpha_1^2 + \beta_3\alpha_1^3)R_1 \\
&\quad + (\beta_1\alpha_2^1 + \beta_2\alpha_2^2 + \beta_3\alpha_2^3)R_2 \\
&\quad + (\beta_1\alpha_3^1 + \beta_2\alpha_3^2 + \beta_3\alpha_3^3)R_3
\end{aligned}
$$

In the above step, we can apply $P_{Q'}$ since the sum of coefficients of $Q_i's$ are 1, and the coefficient of Q_4 is zero. The vertices of S are

$$
\begin{aligned}
S_1 = P_{Q'}(T_1) &= P_{Q'}(\alpha_1^1 Q_1 + \alpha_2^1 Q_2 + \alpha_3^1 Q_3) \\
&= \alpha_1^1 R_1 + \alpha_2^1 R_2 + \alpha_3^1 R_3 \\
S_2 = P_{Q'}(T_2) &= P_{Q'}\alpha_1^2 Q_1 + \alpha_2^2 Q_2 + \alpha_3^2 Q_3) \\
&= \alpha_1^2 R_1 + \alpha_2^2 R_2 + \alpha_3^2 R_3 \\
S_3 = P_{Q'}(T_3) &= P_{Q'}(\alpha_1^3 Q_1 + \alpha_2^3 Q_2 + \alpha_3^3 Q_3) \\
&= \alpha_1^3 R_1 + \alpha_2^3 R_2 + \alpha_3^3 R_3 \\
S_4 = P_{Q'}(T_4) &= P_{Q'}(\alpha_1^4 Q_1 + \alpha_2^4 Q_2 + \alpha_3^4 Q_3) \\
&= \alpha_1^4 R_1 + \alpha_2^4 R_2 + \alpha_3^4 R_3
\end{aligned}
$$

Thus,

$$
\begin{aligned}
P_S(x) &= P_S(\beta_1 Q_1 + \beta_2 Q_2 + \beta_3 Q_3) \\
&= \beta_1 S_1 + \beta_2 S_2 + \beta_3 S_3 \\
&= \beta_1(\alpha_1^1 R_1 + \alpha_2^1 R_2 + \alpha_3^1 R_3) \\
&\quad + \beta_2(\alpha_1^2 R_1 + \alpha_2^2 R_2 + \alpha_3^2 R_3) \\
&\quad + \beta_3(\alpha_1^3 R_1 + \alpha_2^3 R_2 + \alpha_3^3 R_3) \\
&= (\beta_1\alpha_1^1 + \beta_2\alpha_1^2 + \beta_3\alpha_1^3)R_1 \\
&\quad + (\beta_1\alpha_2^1 + \beta_2\alpha_2^2 + \beta_3\alpha_2^3)R_2 \\
&\quad + (\beta_1\alpha_3^1 + \beta_2\alpha_3^2 + \beta_3\alpha_3^3)R_3 \\
&= P_{Q'} \circ P_{Q''}(x)
\end{aligned}
$$

Case 2: Q'' in Δ_2. In this case $\alpha_2^i = 0$ for all $i = 1, 2, 3, 4$ and $P_{Q'} \circ P_{Q''}(x) = P_S(x)$ follows same as in case 1.

Case 3: Q'' along diagonal. Here $\alpha_2^1 = \alpha_4^1 = 0$, $\alpha_2^3 = \alpha_4^3 = 0$, $\alpha_4^2 = 0$ and $\alpha_2^4 = 0$. In this case also, $P_{Q'} \circ P_{Q''}(x) = P_S(x)$ follows same as in case 1. ■

Remark 1: In Proposition 2, the position of Q' does not matter in the calculation.

Remark 2: Proposition 2 is valid only if $Q'' \in \mathcal{S}_m$.

Let $Q = Q_1Q_2Q_3Q_4$, where $Q_1 = (0, 1)$, $Q_2 = (0, 0)$, $Q_3 = (1, 0)$ and $Q_4 = (1, 1)$ and $Q' = R_1R_2R_3R_4$, where $R_1 = (0, \frac{1}{4})$, $R_2 = (0, 0)$, $R_3 = (\frac{1}{4}, 0)$ and $R_4 = (\frac{1}{4}, \frac{1}{4})$ and $Q'' = T_1T_2T_3T_4$, where $T_1 = (\frac{2}{4}, \frac{3}{4})$, $T_2 = (\frac{1}{4}, \frac{1}{4})$, $T_3 = (\frac{3}{4}, \frac{1}{4})$ and $T_4 = (\frac{3}{4}, \frac{3}{4})$. Then,

$$
\begin{aligned}
T_1 &= \frac{1}{2}(0, 1) + 0(0, 0) + \frac{1}{4}(1, 0) + \frac{1}{4}(1, 1) \\
T_2 &= \frac{1}{4}(0, 1) + \frac{1}{2}(0, 0) + \frac{1}{4}(1, 0) + 0(1, 1) \\
T_3 &= \frac{1}{4}(0, 1) + 0(0, 0) + \frac{3}{4}(1, 0) + 0(1, 1) \\
T_4 &= \frac{1}{4}(0, 1) + 0(0, 0) + \frac{1}{4}(1, 0) + \frac{1}{2}(1, 1)
\end{aligned}
$$

Let $x = (\frac{1}{2}, \frac{1}{4}) = \frac{1}{4}(0, 1) + \frac{1}{4}(0, 0) + \frac{1}{2}(1, 0) + 0(1, 1) \in Q$
Hence,

$$
\begin{aligned}
P_{Q'} \circ P_{Q''}(x) &= P_{Q'}(P_{Q''}(\frac{1}{4}(0, 1) + \frac{1}{4}(0, 0) + \frac{1}{2}(1, 0) + 0(1, 1))) \\
&= P_{Q'}(\frac{1}{4}(\frac{2}{4}, \frac{3}{4}) + \frac{1}{4}(\frac{1}{4}, \frac{1}{4}) + \frac{1}{2}(\frac{3}{4}, \frac{1}{4}) + 0(\frac{3}{4}, \frac{3}{4})) \\
&= P_{Q'}(\frac{5}{16}(0, 1) + \frac{1}{8}(0, 0) + \frac{1}{2}(1, 0) + \frac{1}{16}(1, 1))
\end{aligned}
$$

Note that R.H.S. is not well defined. This is because of $Q'' \notin \mathcal{S}_m$.

III. Quadrilateral Labyrinth Fractals

In this section, a set of white quadrilaterals called the labyrinth set, is chosen with some conditions. The corresponding fractal generated from this set is said to be a quadrilateral labyrinth fractal. Besides that, some theorems regarding the labyrinth set and labyrinth fractals have also been proved. Some examples of labyrinth sets are also given. This section requires some basic concepts in graph theory, which are included at the beginning of this section.

A graph $\mathcal{G} = (\mathcal{V}(\mathcal{G}), \mathcal{E}(\mathcal{G}))$ consists of a set of vertices $\mathcal{V}(\mathcal{G})$ and a set of edges $\mathcal{E}(\mathcal{G})$, where $\mathcal{E}(\mathcal{G})$ is a subset of the unordered pairs of $\mathcal{V}(\mathcal{G})$. If $\{v_1, v_2\} \in \mathcal{E}(\mathcal{G})$ then the two vertices v_1 and v_2 are said to be adjacent. A path is a sequence of pairwise distinct vertices $v_1, v_2, \ldots, v_k$, $k \geq 1$ such that for every $j \in \{1, 2, \ldots, k-1\}$, the vertices v_j and v_{j+1} are adjacent. The vertices v_1 and v_k are called the initial and terminal vertices of the path, respectively. If there exists an edge that connects the initial and terminal vertex of a path, then the path is called a cycle (provided that $k > 2$). A graph is said to be connected if a path exists between any two vertices. A connected graph having no cycle is said to be a tree.

For $n \geq 1$, the graph of $\mathcal{W}_n$ is defined as the graph with vertex set $\mathcal{V}(\mathcal{G}(\mathcal{W}_n))$ as the set of white quadrilaterals in $\mathcal{W}_n$ and the edge set $\mathcal{E}(\mathcal{G}(\mathcal{W}_n))$ as the unordered pair of white quadrilaterals in $\mathcal{W}_n$, that have a common side. Such a graph is denoted by $\mathcal{G}(\mathcal{W}_n) = \mathcal{G}(\mathcal{V}(\mathcal{G}(\mathcal{W}_n)), \mathcal{E}(\mathcal{G}(\mathcal{W}_n)))$.

For $n \geq 1$, the graph of $\mathcal{B}_n$ is defined as the graph with vertex set $\mathcal{V}(\mathcal{G}(\mathcal{B}_n))$ as the set of black quadrilaterals in $\mathcal{B}_n$ and the edge set $\mathcal{E}(\mathcal{G}(\mathcal{B}_n))$ as the unordered pair of black quadrilaterals in $\mathcal{W}_n$, that have a common side or a common vertex. Such a graph is denoted by $\mathcal{G}(\mathcal{B}_n) = \mathcal{G}(\mathcal{V}(\mathcal{G}(\mathcal{B}_n)), \mathcal{E}(\mathcal{G}(\mathcal{B}_n)))$.

Definition 2: Let $m \geq 4$ and $\mathcal{W}_1 \subseteq \mathcal{S}_m$. Then $\mathcal{W}_1$ is an $m \times m$ - quadrilateral labyrinth set if it satisfies the following properties:

1) **Tree Property:** $\mathcal{G}(\mathcal{W}_1)$ is a tree.
2) **Exit Property:** There exist exactly one $(k_1, k_2, 0, 0) \in A$ such that $S_m(k_1, k_2, 0, 0) \in \mathcal{W}_1$ and $S_m(0, 0, k_2, k_1) \in \mathcal{W}_1$ and exactly one $(k_1, 0, 0, k_4) \in A$ such that $S_m(k_1, 0, 0, k_4) \in W_1$ and $S_m(0, k_1, k_4, 0) \in W_1$, where A is given as in (1). In this case, $S_m(k_1, k_2, 0, 0)$ is called the left exit, $S_m(0, 0, k_1, k_2)$ is the right exit, $S_m(k_1, 0, 0, k_4)$ is the top exit and $S_m(0, k_1, k_4, 0)$ is the bottom exit.
3) **Corner Property:** If there is a white quadrilateral in $\mathcal{W}_1$ containing any of the vertex $Q_i (i = 1, 2, 3, 4)$ of Q, then the white quadrilateral in $\mathcal{S}_m$ containing the diagonally opposite vertex of Q_i should not be in $\mathcal{W}_1$. i.e. $\mathcal{W}_1$ contains at most one element from each of the sets $\{S_m(m-1, 0, 0, 0), S_m(0, 0, m-1, 0)\}$ and $\{S_m(0, m-1, 0, 0), S_m(0, 0, 0, m-\ 1)\}$.

Definition 3: If $\mathcal{W}_1 \subseteq \mathcal{S}_m$ is a quadrilateral labyrinth set in the quadrilateral Q, the left side of Q is defined as the side of Q which contains the left exit. The right, bottom and top sides of Q are defined analogously. The vertex of Q at the intersection of the top and left side is called the top-left vertex. The top-right vertex, bottom-left vertex and bottom-right vertex are defined analogously. The corner quadrilateral containing the top-left vertex is called the top-left corner. Analogously, the top-right corner, bottom-left corner and bottom-right corner are defined.

Proposition 3: If $\mathcal{W}_1$ is a quadrilateral labyrinth set, no corner can be an exit of two adjacent sides.

Proof: Suppose the result is not valid. WLOG Suppose the bottom-left corner is an exit for both the bottom and left sides. Then, by the exit property, the bottom-right corner is the right exit, and the top-left corner is the top exit, so they belong to $\mathcal{W}_1$. It contradicts the corner property. Thus, no corner can be an exit of two adjacent sides. ■

Proposition 4: If $\mathcal{W}_1$ is an $m \times m$ - quadrilateral labyrinth set, then $\mathcal{W}_n$ is an $m^n \times m^n$ - quadrilateral labyrinth set for all $n \geq 1$.

The proof of the Proposition 4 is the same as the proof in 4×4 labyrinth fractal in a square; hence, the proof is omitted.

Remark 3: For a quadrilateral labyrinth set $\mathcal{W}_1$, it is shown that $\mathcal{G}(\mathcal{W}_n)$ is connected. Hence, L_n is connected for any $n \geq 1$. Thus, $\{L_n\}$ is a decreasing sequence of nonempty compact connected sets.

Definition 4: If $\mathcal{W}_1$ is a quadrilateral labyrinth set, then the limit set $L_\infty = \bigcap_{n=1}^{\infty} L_n = \bigcap_{n=1}^{\infty} \bigcup_{W \in \mathcal{W}_n} W$ is called the quadrilateral labyrinth fractal.

Figs. 2, 3, and 4 show examples of quadrilateral labyrinth fractals.

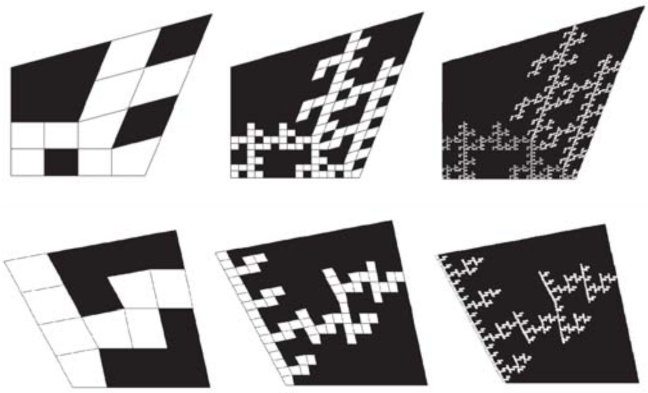

Fig. 2 First three stages of two different 4×4-quadrilateral labyrinth fractals

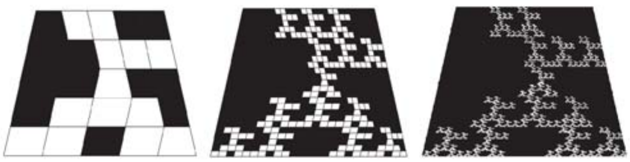

Fig. 3 First three stages of a 5×5-quadrilateral labyrinth fractal

Fig. 4 First three stages of a 6×6-quadrilateral labyrinth fractal

Proposition 5: Let $\mathcal{W}_1$ be a quadrilateral labyrinth set in the quadrilateral Q. Then for any integer $n \geq 1$,
$\mathcal{W}_n = \{P_{W_1^1, W_1^2, \ldots, W_1^n}(Q) : W_1^i \in \mathcal{W}_1 \ \forall \ i = 1, 2, \ldots, n\}$,
where, $P_{W_1^1, W_1^2, \ldots, W_1^n} = P_{W_1^1} \circ P_{W_1^2} \circ \ldots \circ P_{W_1^n}$.

Proof: The proof is by induction. For $n = 1$, it is clear that $\mathcal{W}_1 = \{P_{W_1}(Q) : W_1 \in \mathcal{W}_1\}$. So, the result is true for $n = 1$. Suppose the result holds up to $n - 1$. i.e.,
$\mathcal{W}_{n-1} = \{P_{W_1^1, W_1^2, \ldots, W_1^{n-1}}(Q) : W_1^i \in \mathcal{W}_1, \ \forall \ i = 1, 2, \ldots, n-1\}$.

Let $\mathcal{V}_n = \{P_{W_1^1,W_1^2,\ldots,W_1^n}(Q) : W_1^i \in \mathcal{W}_1 \ \forall\ i = 1,2,\ldots,n\}$. It is enough to prove that $\mathcal{W}_n = \mathcal{V}_n$, where $\mathcal{W}_n$ is given as $\mathcal{W}_n = \{P_{W_{n-1}}(W_1) : W_1 \in \mathcal{W}_1, W_{n-1} \in \mathcal{W}_{n-1}\}$.

Choose an element $P_{W_{n-1}}(W_1) \in \mathcal{W}_n$. Then $P_{W_{n-1}}(W_1) = P_{W_{n-1}} \circ P_{W_1}(Q) \in \mathcal{W}_n$. By induction hypothesis $W_{n-1} = P_{W_1^1,W_1^2,\ldots,W_1^{n-1}}(Q)$ for $W_1^i \in \mathcal{W}_1,\ \forall\ i = 1,2,\ldots,n-1$. Using Proposition 2 recursively,

$$\begin{aligned}P_{W_{n-1}}(W_1) &= P_{W_{n-1}} \circ P_{W_1}(Q)\\ &= P_{P_{W_1^1,W_1^2,\ldots,W_1^{n-1}}(Q)} \circ P_{W_1}(Q)\\ &= P_{W_1^1} \circ P_{W_1^2} \circ \ldots \circ P_{W_1^{n-1}} \circ P_{W_1}(Q)\end{aligned}$$

Thus $\mathcal{W}_n \subseteq V_n$.

If $\mathcal{W}_1$ contains k elements, then clearly the number of elements in $\mathcal{W}_n$ and $\mathcal{V}_n$ are k^n. Hence $\mathcal{W}_n = \mathcal{V}_n$ ■

Proposition 6: For all $n \geq 1$, $L_\infty = \bigcup_{W_n \in \mathcal{W}_n} P_{W_n}(L_\infty)$

Proof: Using continuity of P_{W_n} and Proposition 5, it can be easily shown that $P_{W_n}(L_\infty) = W_n \cap L_\infty$, for any $n \geq 1$. Hence,

$$\begin{aligned}\bigcup_{W_n \in \mathcal{W}_n} P_{W_n}(L_\infty) &= \bigcup_{W_n \in \mathcal{W}_n} (W_n \cap L_\infty)\\ &= L_\infty \cap \bigcup_{W_n \in \mathcal{W}_n} W_n\\ &= L_\infty \cap L_n = L_\infty\end{aligned}$$

■

IV. Condition for the Contractivity of Maps between Quadrilaterals

This section examines whether the map between two quadrilaterals is a contraction or not. It is found that under certain conditions, the maps between quadrilaterals are contraction, and in such cases, the contraction ratio is also examined. Besides that, these conditions give the class of quadrilateral labyrinth fractal, which can be generated from an iterated function system.

Let $Q = Q_1Q_2Q_3Q_4$ and $R = R_1R_2R_3R_4$ be two convex quadrilaterals with the following properties.

1) $\frac{d(R_1,R_2)}{d(Q_1,Q_2)} < 1$, $\frac{d(R_2,R_3)}{d(Q_2,Q_3)} < 1$, $\frac{d(R_3,R_4)}{d(Q_3,Q_4)} < 1$, $\frac{d(R_4,R_1)}{d(Q_4,Q_1)} < 1$
2) The smallest diagonal of Q is Q_1Q_3, if and only if the smallest diagonal of R is R_1R_3.
3) $\frac{\text{length of the smallest diagonal of R}}{\text{length of the smallest diagonal of Q}} < 1$

The map $P_R : Q \to R$ given by Definition 1 need not be a contraction for all Q and R even though Q and R satisfy the above three conditions.

Example 1: Consider $Q = Q_1Q_2Q_3Q_4$ and $R = R_1R_2R_3R_4$ as in Fig. 5.

Note $\frac{d(R_1,R_2)}{d(Q_1,Q_2)} = 0.884 < 1$, $\frac{d(R_2,R_3)}{d(Q_2,Q_3)} = 0.875 < 1$, $\frac{d(R_3,R_4)}{d(Q_3,Q_4)} = 0.14 < 1$, $\frac{d(R_4,R_1)}{d(Q_4,Q_1)} = 0.14 < 1$ and $\frac{d(R_1,R_3)}{d(Q_1,Q_3)} = 0.088 < 1$. The smallest diagonal of Q is Q_1Q_3, and that of R is R_1R_3. Thus, all the three conditions above are satisfied. But the map $P_R : Q \to R$ is not contraction.

Consider the point $z = (4,4) \in Q$. Its unique representation is $(\frac{1}{2}, 0, \frac{1}{2}, 0)$. i.e., $z = (4,4) = \frac{1}{2}Q_1 + 0Q_2 + \frac{1}{2}Q_3 + 0Q_4$. Thus,

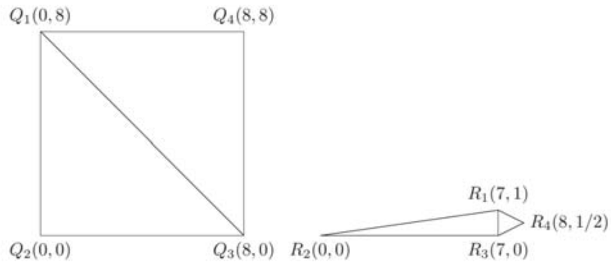

Fig. 5 $Q = Q_1Q_2Q_3Q_4$ and $R = R_1R_2R_3R_4$

$P_R(z) = P_R(\frac{1}{2}Q_1 + 0Q_2 + \frac{1}{2}Q_3 + 0Q_4) = \frac{1}{2}R_1 + 0R_2 + \frac{1}{2}R_3 + 0R_4 = (7, \frac{1}{2})$. But, $d(P_R(z), P_R(Q_2)) = 7.02 > d(z, Q_2) = 5.657$. i.e., P_R is not a contraction.

Theorem 1: [10] Let $\Delta = ABC$ and $\delta = A'B'C'$ be triangles in $\mathbb{R}^2$ with vertices $\{(0,0),(a,0),(b_1,b_2)\}$ and $\{(0,0),(a',0),(b_1',b_2')\}$ respectively. Let $P_\delta : \Delta \to \delta$ be a linear transformation sending A to A', B to B' and C to C'. Then P_δ is a contraction if $\lambda_1 = \sqrt{(k+m)^2 + \theta^2(l-k)^2} + \sqrt{(k-m)^2 + \theta^2(l-k)^2} < 2$ where, $k = \frac{a'}{a}, l = \frac{b_1'}{b_1}, m = \frac{b_2'}{b_2}, \theta = \frac{b_1}{b_2}$ and in this case the contraction ratio is $\lambda = \frac{\lambda_1}{2}$

Remark 4: Let Δ_1 be a triangle with coordinates $A_1 = (a_1,b_1), A_2 = (a_2,b_2), A_3 = (a_3,b_3)$, and Δ_2 be a triangle obtained from Δ_1 by translation and rotation such that one vertex of Δ_2 is at origin $P_1 = (0,0)$ and another vertex P_2 at $(p,0)$. Let the third vertex of Δ_2 is given by $P_3 = (r_1,r_2)$. Assume A_1 is mapped to $P_1 = (0,0)$ and A_2 is mapped to $P_2 = (p,0)$. Since translation and rotation do not change the distance between two points, $d(A_1,A_2) = d(P_1,P_2)$ which gives $p = \sqrt{(a_1-a_2)^2 + (b_1-b_2)^2}$. Also, $d(A_1,A_3) = d(P_1,P_3)$ and $d(A_2,A_3) = d(P_2,P_3)$ implies $(a_1-a_3)^2 + (b_1-b_3)^2 = r_1^2 + r_2^2$ and $(a_2-a_3)^2 + (b_2-b_3)^2 = (p-r_1)^2 + r_2^2$. Substituting the value of p and simplifying the above equations, the value of r_1 and r_2 are obtained as follows:

$$\begin{aligned}r_1 &= \frac{(a_1-a_2)^2 + (b_1-b_2)^2 + (a_1-a_3)^2}{2\sqrt{(a_1-a_2)^2 + (b_1-b_2)^2}}\\ &\quad + \frac{(b_1-b_3)^2 - (a_2-a_3)^2 - (b_2-b_3)^2}{2\sqrt{(a_1-a_2)^2 + (b_1-b_2)^2}}\\ &= \frac{(a_1^2 - a_1a_2 + a_2a_3 - a_3a_1 + b_1^2 - b_1b_2 + b_2b_3 - b_3b_1)}{\sqrt{(a_1-a_2)^2 + (b_1-b_2)^2}}\\ r_2 &= \sqrt{(a_1-a_3)^2 + (b_1-b_3)^2 - r_1^2}\end{aligned}$$

Hence, the coordinates of Δ_2 are obtained.

The above remark helps us formulate the conditions on quadrilateral so that the map $P_R : Q \to R$ is contraction.

Theorem 2: Let $Q = Q_1Q_2Q_3Q_4$ be a quadrilateral with smallest diagonal Q_1Q_3, $R = R_1R_2R_3R_4$ be another quadrilateral with smallest diagonal R_1R_3, and $P_R : Q \to R$ be the map between quadrilaterals as in Definition 1. Also, let $Q_i = (a_i,b_i)$ and $R_i = (c_i,d_i)$ for $i = 1,2,3,4$. Take $\Delta_1 = Q_1Q_2Q_3$, $\Delta_2 = Q_3Q_4Q_1$, $\delta_1 = R_1R_2R_3$, and $\delta_2 = R_3R_4R_1$. Then, P_R is a contraction if the following two conditions are satisfied.

$$\lambda_1 = \sqrt{(k_1+m_1)^2 + \theta_1^2(l_1-k_1)^2} + \sqrt{(k_1-m_1)^2 + \theta_1^2(l_1-k_1)^2} < 2$$

$$\lambda_2 = \sqrt{(k_2+m_2)^2 + \theta_2^2(l_2-k_2)^2} + \sqrt{(k_2-m_2)^2 + \theta_2^2(l_2-k_2)^2} < 2$$

where the values of $k_1, m_1, l_1, \theta_1, k_2, m_2, l_2$, and θ_2 are as given in Appendix **??**. The contraction ratio of P_R is $\lambda = max\{\frac{\lambda_1}{2}, \frac{\lambda_2}{2}\}$

Proof: **Case 1:** $x, y \in \Delta_1$ or $x, y \in \Delta_2$
Then, $x = \alpha_1 Q_1 + \alpha_2 Q_2 + \alpha_3 Q_3 + 0Q_4$ with $\alpha_1+\alpha_2+\alpha_3 = 1$, and $y = \beta_1 Q_1 + \beta_2 Q_2 + \beta_3 Q_3 + 0Q_4$ with $\beta_1+\beta_2+\beta_3 = 1$ or $x = \alpha_1 Q_1 + 0Q_2 + \alpha_3 Q_3 + \alpha_4 Q_4$ with $\alpha_1+\alpha_3+\alpha_4 = 1$, and $y = \beta_1 Q_1 + 0Q_2 + \beta_3 Q_3 + \beta_4 Q_4$ with $\beta_1+\beta_3+\beta_4 = 1$. Then $P_R(x) = \alpha_1 R_1 + \alpha_2 R_2 + \alpha_3 R_3 + 0R_4$ and $P_R(y) = \beta_1 R_1 + \beta_2 R_2 + \beta_3 R_3 + 0R_4$ or $P_R(x) = \alpha_1 R_1 + 0R_2 + \alpha_3 R_3 + \alpha_4 R_4$ and $P_R(y) = \beta_1 R_1 + 0R_2 + \beta_3 R_3 + \beta_4 R_4$. In both cases P_R reduces to a linear map from Δ_1 to δ_1 or Δ_2 to δ_2. So, by Theorem 1, $d(P_R(x), P_R(y)) \leq \frac{\lambda_i}{2} d(x,y) \leq \lambda d(x,y)$ for $i = 1$ or 2.

Case 2: $x \in \Delta_1, y \in \Delta_2$ or $x \in \Delta_2, y \in \Delta_1$. Then $P_R(x) \in \delta_1$, $P_R(y) \in \delta_2$ or $P_R(x) \in \delta_2$, $P_R(y) \in \delta_1$ respectively. Let p be the point in the smallest diagonal of Q at which the line from x to y intersects with the smallest diagonal.

Suppose $p = \gamma_1 Q_1 + 0Q_2 + \gamma_3 Q_3 + 0Q_4$, with $\gamma_1 + \gamma_3 = 1$. Then $P_R(p) = \gamma_1 R_1 + 0R_2 + \gamma_3 R_3 + 0R_4$ is a point in the smallest diagonal of R. So, $d(P_R(x), P_R(y)) \leq d(P_R(x), P_R(p)) + d(P_R(p), P_R(y)) \leq \frac{\lambda_1}{2} d(x,p) + \frac{\lambda_2}{2} d(p,y)$ or $\frac{\lambda_2}{2} d(x,p) + \frac{\lambda_1}{2} d(p,y) \leq \lambda(d(x,p) + d(p,y)) = \lambda d(x,y)$. Hence $P_R : Q \to R$ is contraction map from Q to R with contraction ratio λ. ∎

Theorem 3: Let L_∞ be a labyrinth fractal generated from the convex quadrilateral Q. Also, suppose $\mathcal{W}_1$ is the set of first stage white quadrilaterals of L_∞. If each of the map from the set $\{P_{W_1} : Q \to W_1; W_1 \in \mathcal{W}_1\}$ satisfies the Theorem 2, then L_∞ is an attractor of the iterated function system $\{P_{W_n} : W_n \in \mathcal{W}_n\}$ for any n.

Proof: If each of the map from the set $\{P_{W_1} : Q \to W_1; W_1 \in \mathcal{W}_1\}$ satisfies the Theorem 2, then each P_{W_1} is a contraction. Hence, its restriction to the subset L_∞ is again a contraction. It is clear from Proposition 5 that each P_{W_n} can be written as the composition of n number of P_{W_1} maps, where W_1 varies in $\mathcal{W}_1$. Since each P_{W_1} is a contraction, the composition map P_{W_n} is also a contraction. Hence by Proposition 6, L_∞ is an attractor of the iterated function system $\{P_{W_n} : W_n \in \mathcal{W}_n\}$ for any n. ∎

V. Box-Counting Dimension

This section gives the box-counting dimension of quadrilateral labyrinth fractals. The box-counting dimension is found by finding an upper bound and lower bound of the number of boxes required to cover the fractal at each stage.

Let L_∞ be an $m \times m$ quadrilateral labyrinth fractal generated from an $m \times m$ quadrilateral labyrinth set $\mathcal{W}_1$ inside a quadrilateral $Q = Q_1Q_2Q_3Q_4$. Suppose number of elements in $\mathcal{W}_1$ is k. Let $l = max\{d(Q_1,Q_2), d(Q_2,Q_3), d(Q_3,Q_4), d(Q_4,Q_1)\}$. WLOG, suppose that $l = d(Q_1,Q_2)$. An example of such a quadrilateral is given in Fig. 6.

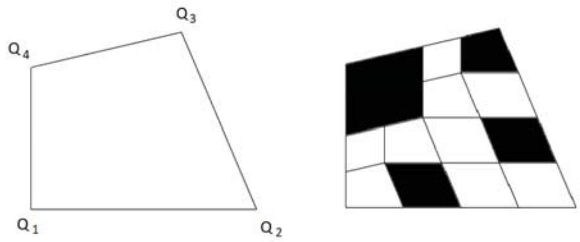

Fig. 6 (a) A quadrilateral (b) first stage of a $4 \times 4-$ quadrilateral labyrinth fractal

Let N_n denote the number of squares of side length $\frac{l}{m^n}$, which covers the n^{th} stage, $\mathcal{W}_n$, of L_∞.
Claim 1: $N_1 \leq 2k$
To prove the Claim 1, it is enough to show that each element in $\mathcal{W}_1$ can be covered by at most two squares of side length $\frac{l}{m}$. Let $R = R_1R_2R_3R_4$ be an element of $\mathcal{W}_1$. Then R can be either in any of the sets $S_m(A_1), S_m(A_2)$, or $S_m(A_3)$.

Case 1: If $R \in S_m(A_1)$, then R is a parallelogram with side lengths $d(R_1,R_2) = d(R_3,R_4) = \frac{d(Q_1,Q_2)}{m}$ and $d(R_2,R_3) = d(R_4,R_1) = \frac{d(Q_2,Q_3)}{m}$. Since $d(Q_1,Q_2) = l$, $d(R_1,R_2) = d(R_3,R_4) = \frac{l}{m}$ and $d(R_2,R_3) = d(R_4,R_1) \leq \frac{l}{m}$. Now, one square of side length $\frac{l}{m}$ is placed on the side R_1R_2 and another on the side R_3R_4 such that R is covered. Depending on the original quadrilateral Q, the two kinds of covering can occur as in Fig. 7.

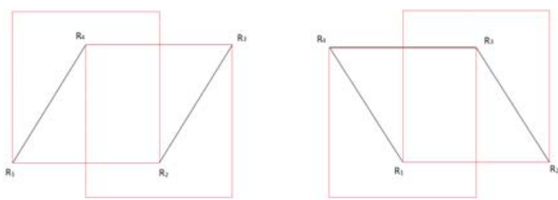

Fig. 7 Two kinds of covering squares for elements in $S_m(A_1)$

Note that these two squares are enough to cover R since R is a parallelogram, and the side R_1R_2 is the side of the largest length, and because of the same reason, it is clear that the covering will never be as in Fig. 8.

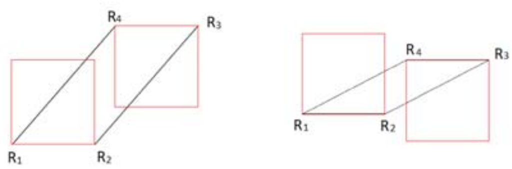

Fig. 8 No such coverings

Case 2: If $R \in S_m(A_2)$, then R is a parallelogram with side lengths $d(R_1,R_2) = d(R_3,R_4) = \frac{d(Q_3,Q_4)}{m}$

and $d(R_2, R_3) = d(R_4, R_1) = \frac{d(Q_4,Q_1)}{m}$. Since $d(Q_3, Q_4) \leq l$ and $d(Q_4, Q_1) \leq l$, $d(R_1, R_2) = d(R_3, R_4) \leq \frac{l}{m}$ and $d(R_2, R_3) = d(R_4, R_1) \leq \frac{l}{m}$. So two squares of side length $\frac{l}{m}$ will cover R as depicted in Fig. 9.

Case 3: If $R \in S_m(A_3)$, then R is similar to Q with similarity ratio $\frac{1}{m}$. Since $d(Q_1, Q_2) = l$, $d(R_1, R_2) = \frac{l}{m}$ and R_1R_2 is the side of maximum length of R. So, the angle at R_1 and R_2 cannot be obtuse. Otherwise, the length of R_3R_4 will be greater than R_1R_2. Suppose the angle at R_1 is not obtuse. Then one square of side length $\frac{l}{m}$ is placed on the side R_1R_2 and the second square is placed with one vertex at R_2 as shown in Fig. 10 so that these two squares cover the quadrilateral R.

Hence, each quadrilateral in $\mathcal{W}_1$ is covered by at most two squares of side length $\frac{l}{m}$. So, $N_1 \leq 2k$.

Note that the n^{th} stage $\mathcal{W}_n$ of L_∞ is an $m^n \times m^n-$quadrilateral labyrinth set and $\mathcal{W}_n$ contains k^n elements, when $\mathcal{W}_1$ contains k elements. Hence $N_n \leq 2k^n$ and so $logN_n \leq log2k^n$. For sufficiently large n,

$$\frac{\log N_n}{-\log(l/m^n)} \leq \frac{\log(2k^n)}{-\log(l/m^n)}$$
$$\implies \frac{\log N_n}{-\log(l/m^n)} \leq \frac{\log(2k^n)}{\log m^n - \log l}$$
$$\implies \frac{\log N_n}{-\log(l/m^n)} \leq \frac{\log(2) + \log(k^n)}{\log m^n - \log l}$$
$$\implies \frac{\log N_n}{-\log(l/m^n)} \leq \frac{\log 2}{n \log m - \log l} + \frac{\log(k)}{\log m - \frac{\log l}{n}}$$

Thus,

$$\lim_{n\to\infty} \frac{\log N_n}{-\log(l/m^n)} \leq \frac{\log(k)}{\log m} \tag{2}$$

Hence, the box-counting dimension of an $m \times m$ quadrilateral labyrinth fractal L_∞ is bounded above by $\frac{\log k}{\log m}$, where k is the number of elements in $\mathcal{W}_1$.

Now, choose a positive number l' such that there exists a square of length $\frac{l'}{m}$ inside each element of $\mathcal{W}_1$. Consider the covering of n^{th} stage of L_∞ by squares of length $\frac{l'}{m^n}$. Let N'_n be the number of squares of length $\frac{l'}{m^n}$ used to cover the n^{th} stage. Then,

Claim: $k^n \leq N'_n$

For $n = 1, k \leq N'_1$ is obvious. For $n > 1$, it is enough to prove that corresponding to each $W \in \mathcal{W}_n$, there exists a square of length $\frac{l'}{m^n}$, which is completely inside W. Note that, each element in $\mathcal{W}_n$ is similar to any one of the element in $\mathcal{W}_1$ with similarity ratio $\frac{1}{4^{n-1}}$ and a square of side length $\frac{l'}{m^n}$ is similar to a square of side length $\frac{l'}{m}$ with similarity ratio $\frac{1}{4^{n-1}}$. So, clearly, each element in $\mathcal{W}_n$ contains a square of side length $\frac{l'}{m^n}$. Hence $k^n \leq N'_n$ for all $n \in \mathbb{N}$. For sufficiently large n,

$$\frac{\log(k^n)}{-\log(l'/m^n)} \leq \frac{\log N'_n}{-\log(l'/m^n)}$$
$$\implies \frac{\log(k^n)}{\log(m^n) - \log(l')} \leq \frac{\log N'_n}{-\log(l'/m^n)}$$
$$\implies \frac{\log k}{\log m - \frac{\log(l')}{n}} \leq \frac{\log N'_n}{-\log(l'/m^n)}$$

Thus,

$$lim_{n\to\infty} \frac{\log N_n}{-\log(l/m^n)} \geq \frac{\log(k)}{\log m} \tag{3}$$

Hence, the box-counting dimension of an $m \times m$ quadrilateral labyrinth fractal, L_∞ is bounded below by $\frac{\log k}{\log m}$, where k is the number of elements in $\mathcal{W}_1$. By (2) and (3), it is clear that the box-counting dimension of an $m \times m$ quadrilateral labyrinth fractal is $\frac{\log k}{\log m}$ where k is the number of elements in $\mathcal{W}_1$.

VI. Hausdorff Dimension

This section deals with the Hausdorff dimension of the quadrilateral labyrinth fractals. The monotonicity property is used to find the lower bound of the Hausdorff dimension. It is seen that the lower bound of the Hausdorff dimension and the box-counting dimension are equal, and it ensures that the box-counting and Hausdorff dimensions of the quadrilateral labyrinth fractal are equal.

Let Q be a convex quadrilateral and L_∞ be the labyrinth fractal generated from a labyrinth set $\mathcal{W}_1 \subseteq \mathcal{S}_m = \mathcal{S}_m(A_1) \cup \mathcal{S}_m(A_2) \cup \mathcal{S}_m(A_3)$ where $\mathcal{S}_m, A_1, A_2, A_3$ are all defined as in Section II. Choose $W_1 \in \mathcal{W}_1$ such that $W_1 \in S_m(A_1) \bigcup S_m(A_2)$ (i.e, W_1 is a parallelogram). Then $W_1 \cap L_\infty \subseteq L_\infty$ and $dim_H(W_1 \cap L_\infty) \leq dim_H(L_\infty)$. Also, note that $W_1 \cap L_\infty$ can be seen as a labyrinth fractal constructed on the parallelogram W_1, with its initial labyrinth set containing the same number of white quadrilaterals as that of $\mathcal{W}_1$ and the position of these white quadrilaterals are same as the position of W_1s in Q. That means the Hausdorff dimension of a labyrinth fractal in a parallelogram forms a lower bound for the Hausdorff dimension of a quadrilateral labyrinth fractal. So, it is enough to concentrate on the Hausdorff dimension of a labyrinth fractal in a parallelogram. For simplicity, let R denote the parallelogram.

Definition 5: A geometric graph directed construction in $\mathbb{R}^m$ consists of

1) A finite sequence of non-overlapping, compact subsets of $\mathbb{R}^m$, say, $W_1, W_2, \ldots, W_k$ such that each W_i has a nonempty interior.
2) A directed graph G with vertex set consisting of the integers $1, 2, \ldots, k$ and similarity maps $T_{i,j}$ of $\mathbb{R}^m$, where $(i, j) \in G$, with similarity ratios $t_{i,j}$ such that
   a) for each i, $1 \leq i \leq k$, there is some j such that $(i, j) \in G$.
   b) for each i, $\{T_{i,j}(W_j) : (i, j) \in G\}$ is a non-overlapping family and $W_i \supset \cup\{T_{i,j}(W_j) : (i, j) \in G\}$.
   c) if the path component of G rooted at the vertex i_1 is a cycle $[i_1, i_2, \ldots i_q, i_{q+1} = i_1]$, then $\Pi_{k=1}^{q} t_{i_k i_{k+1}} < 1$

$\{W_1, W_2, \ldots, W_k\}$ is taken as the white parallelograms in the first stage of labyrinth fractal constructed on R, where k is the number of white quadrilaterals of the first stage. Consider the directed graph G as a graph with vertex set $\{1, 2, \ldots, k\}$ and edge set $\{(1, 1), (1, 2), \ldots, (1, k), (2, 1), (2, 2), \ldots, (2, k), \ldots, (k, 1), (k, 2), \ldots, (k, k)\}$. Corresponding to each (i, j), where, $i, j =$

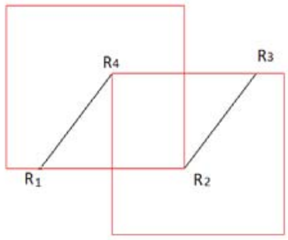

Fig. 9 Two kinds of covering squares for elements in $S_m(A_2)$

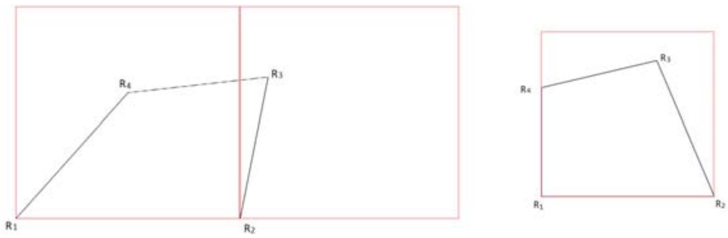

Fig. 10 Two kinds of covering squares for elements in $S_m(A_3)$

$1, 2, .., k$, take, $T_{i,j}(x) = P_{W_i}(x)$ for all j, and so $t_{i,j} = \frac{1}{m}$ for all i and j.

Theorem 4: [11] For each geometric construction, there exists a unique vector of compact sets, $(K_1, K_2, \dots K_k) \in \Pi_{i=1}^{k}\mathcal{K}(W_i)$ such that for each i, $W_i = \bigcup\{T_{i,j}(W_j) : (i,j) \in G\}$, where $\mathcal{K}(W_i)$ denotes the space of compact subsets of W_i. The construction object of this geometric construction is defined as $K = \bigcup_{i=1}^{k} K_i$.

Definition 6: The weighted incidence matrix or construction matrix $A = A_G$ associated with a graph directed construction is the $k \times k$ matrix defined by $A = [t_{i,j}]_{1 \le i,j \le k}$, where we make the convention that $t_{i,j} = 0$ if $(i,j) \notin G$. For each $\beta \ge 0$, let $A_\beta = A_{G,\beta}$ be the $k \times k$ matrix given by $a_{\beta;i,j} = t_{i,j}^{\beta}$. $\Phi(\beta)$ denotes the spectral radius of A_β.

Mauldin and Williams introduced the graph-directed construction and examined the Hausdorff dimension of the construction object obtained from this construction [11].

Theorem 5: [11] For each graph-directed construction such that G itself is strongly connected, the Hausdorff dimension of K, the construction object, is α, where $\Phi(\alpha) = 1$.

The labyrinth fractal in the parallelogram can be seen as the construction object of the graph-directed construction with the weighted incidence matrix, $A = [\frac{1}{m}]_{k \times k}$. For any $\beta > 0$, A_β is a matrix having all entries equal. So, it is easy to see that $\Phi(\beta)$ of A_β is the sum of row entries. So, it is enough to find the value of β for which this sum of row elements equals one, i.e., the Hausdorff dimension β is such that $\Sigma_{i=1}^{k}(\frac{1}{m})^{\beta} = 1 \implies \beta = \frac{\log k}{\log m}$. So, for any $m \times m$ labyrinth fractal generated on a parallelogram, Hausdorff dimension is equal to $\frac{\log k}{\log m}$, where k is the number of white parallelograms of stage 1. Since the box-counting dimension of $m \times m$ quadrilateral labyrinth fractal is obtained as $\frac{\log k}{\log m}$, it can be seen that the Hausdorff dimension of $m \times m$ quadrilateral labyrinth fractal is $\frac{\log k}{\log m}$, where k is the number of white quadrilaterals of stage 1.

VII. Topological Properties

This section deals with the topological properties of the labyrinth set and labyrinth fractal. The section also studies different connectedness properties in $Q \setminus L_n$ and $Q \setminus L_\infty$. It can be seen that many of the results in $m \times m$ labyrinth fractal in a square are satisfied for a quadrilateral labyrinth fractal, too. So we state the Propositions 7 and 8 and Theorem 6 without proofs.

Proposition 7: If $\mathcal{W} \subset \mathcal{S}_m$ is a set of white quadrilaterals such that the associated graph $\mathcal{G}(\mathcal{W})$ is a tree. From every black quadrilateral in $\mathcal{B} = \mathcal{S}_m \setminus \mathcal{W}$, there is a path in $\mathcal{G}(\mathcal{B})$ to a border quadrilateral.

Definition 7: Let X be a topological space and $x_0, x_1 \in X$. Then an arc in X from x_0 to x_1 is a continuous function $\gamma : [0,1] \to X$ such that $\gamma(0) = x_0$ and $\gamma(1) = x_1$.

Definition 8: A dendrite is a locally connected continuum that contains no simple closed curve, and a continuum is a nonempty compact connected Hausdorff space.

Proposition 8: If x is a point in $Q \setminus L_n$, then there is an arc $a \subseteq Q \setminus L_{n+1}$ between x and a point in the boundary of Q.

Corollary 1: If x is a point in $Q \setminus L_\infty$, then there is an arc $a \subseteq Q \setminus L_\infty$ between x and a point in the boundary of Q.

Theorem 6: L_∞ is a dendrite.

Theorem 7: The interior of L_∞ is empty.

Proof: Suppose not. Then there exist a point $x \in \text{Int}(L_\infty)$ and an $r > 0$ such that ball with center x and radius r, say $\underline{B(x,r)}$, is contained in L_∞. Choose an ϵ such that $o < \epsilon < r$ and $\overline{B(x,\epsilon)} \subseteq B(x,r)$. Then clearly, the circle with centre x and radius ϵ is a simple closed curve contained in L_∞. It is a contradiction. ■

Corollary 2: L_∞ is a first category subset in $\mathbb{R}^2$.

Proof: Since L_∞ is closed, the interior of closure of L_∞ is the same as the interior of L_∞ and it is empty. Thus L_∞ is nowhere dense subset of $\mathbb{R}^2$.

Consider closed intervals in $\mathbb{R}$ with rational endpoints and then consider a strip on $\mathbb{R}^2$ corresponding to each of these intervals. i.e, if $[r_1, r_2]$ is a interval with $r_1, r_2 \in \mathbb{Q}$, consider the strip $[r_1, r_2] \times y - axis$. Collection of all such strips is, say, $\{A_i\}$, is countable. Let $B_i = A_i \cap L_\infty$. Then $\{B_i\}$ is countable and $L_\infty = \bigcup_{i=1}^{\infty} B_i$ and each B_i is nowhere dense since they are subsets of nowhere dense set L_∞. Hence, L_∞ is the first category subset in $\mathbb{R}^2$. ■

Remark 5: Let L_∞ as a subspace of $\mathbb{R}^2$ with induced Topology. Then L_∞ is compact and Hausdorff, hence a Baire's space. Since every Baire space is of the second category, L_∞ is the second category subspace [12].

Theorem 8: $Q \setminus L_\infty$ is not path connected.

Proof: Choose an exit W_L of $\mathcal{W}_1$ such that W_L is not a corner quadrilateral. Such an exit always exists by Proposition 3 and corner property. WLOG suppose that W_L is the left exit and let P be a path from W_L to W_R, where W_R is the right exit of $\mathcal{W}_1$, which is not a corner quadrilateral. Let $a = L_\infty \cap P$. Then a is a path from left to right exit in L_∞. Since both the bottom-left and bottom-right corners cannot be white in $\mathcal{W}_1$, choose the black quadrilateral, say B, from these corners. Similarly, choose a black quadrilateral, say B', from the top-left and top-right corners of $\mathcal{W}_1$. Let $x \in B$ and $y \in B'$. Now, if a path exists from x to y, it should intersect with a, which is impossible since $a \subseteq L_\infty$. So there does not exist a path from x to y in $Q \setminus L_\infty$, so $Q \setminus L_\infty$ is not path connected. ■

Corollary 3: $Q \setminus L_\infty$ is not connected.

Proof: Claim: $Q \setminus L_\infty$ is locally path connected.
Let $x \in Q \setminus L_\infty$, and U is an open set containing x. For sufficiently small r, there exists an open ball containing x and contained in U in subspace topology, and it will be path connected. Hence, $Q \setminus L_\infty$ is locally path connected. Since every locally path-connected space is connected if and only if the space is path-connected, $Q \setminus L_\infty$ is not connected by Theorem 8. ■

Corollary 4: $Q \setminus L_n$ is not path connected and not connected for any $n \geq 1$.

Theorem 9: If $\mathcal{W}_1$ is an $m \times m$ - quadrilateral labyrinth set in Q, $m \geq 4$, such that $\mathcal{W}_1$ contains no border quadrilateral except the exits, and L_∞ is the quadrilateral labyrinth fractal generated from $\mathcal{W}_1$, then the number of connected components of $Q \setminus L_\infty$ is 4.

Proof: Claim 1: $\mathcal{W}_1$ cannot have a corner quadrilateral.

Suppose a corner quadrilateral exists, say W_0 in $\mathcal{W}_1$. Let W_0 be the top-left corner. Then, it should be either left-exit or top-exit. WLOG suppose W_0 is the top-exit. Since $\mathcal{W}_1$ is connected, there exists a border quadrilateral, say W_1, which is a neighbour of W_0. Since W_1 is a border quadrilateral, it should be an exit. Also, W_1 cannot be a top exit, so W_1 is a left exit. Since the top-left corner is the top exit, the bottom-left corner should be the bottom exit. Same argument as above, a left exit exists, say W_2, a neighbour of the bottom left corner. Since the left exit is unique, the only possibility is $W_1 = W_2$. But this case holds only if $m = 3$. So $\mathcal{W}_1$ contains no corner quadrilateral. Hence each vertex of Q is in $Q \setminus L_\infty$.

Claim 2: A connected component of $Q \setminus L_\infty$ does not contain more than one vertex of Q.

Suppose not. Let K be a connected component of $Q \setminus L_\infty$ which contains two corner vertices. WLOG assume the top-left vertex and top-right vertex are contained in K. Since $Q \setminus L_\infty$ is locally path connected, the path connected components and connected components of $Q \setminus L_\infty$ coincide. Thus, K is a path-connected component containing both the top-left vertex and the top-right vertex, and a path exists in K between these two vertices. But this path will intersect with the path from top exit to bottom exit as shown in Theorem 6, and it is not possible. Hence, a connected component of $Q \setminus L_\infty$ contains at most one vertex of Q.

Claim 3: Each connected component of $Q \setminus L_\infty$ contains at least one vertex.

From Corollary 1, it is clear that there exists a path from any point of $Q \setminus L_\infty$ to one of the boundary points of Q. Also, from any border point in $Q \setminus L_n$, a path exists to one of the vertices of Q; otherwise, it will contradict the theorem hypothesis. Hence, each component of $Q \setminus L_n$ contains at least one vertex of Q. Thus, corresponding to each vertex is a unique connected component in $Q \setminus L_\infty$, so the number of related components of $Q \setminus L_\infty$ is 4. ■

VIII. Conclusion

In this paper, labyrinth fractals on a convex quadrilateral are introduced. Labyrinth fractals are defined in the same manner as in a square or a triangle on any convex quadrilateral. However, the labyrinth fractal is not self-similar as the construction of smaller quadrilaterals lacks self-similarity property.

The Hausdorff dimension and the box-counting dimension of the constructed quadrilateral labyrinth fractals are obtained, and it is observed that both dimensions coincide. The topological properties of the quadrilateral labyrinth fractal and its complement on the quadrilateral are also studied in this paper.

Acknowledgment

The first author was supported by a PMRF grant.

APPENDIX

$$k_1 = \frac{\sqrt{(c_1-c_2)^2+(d_1-d_2)^2}}{\sqrt{(a_1-a_2)^2+(b_1-b_2)^2}}$$

$$m_1 = \frac{\sqrt{((c_1-c_3)^2+(d_1-d_3)^2)((c_1-c_2)^2+(d_1-d_2)^2)-(c_1^2-c_1c_2+c_2c_3-c_3c_1+d_1^2-d_1d_2+d_2d_3-d_3d_1)^2}\sqrt{(a_1-a_2)^2+(b_1-b_2)^2}}{\sqrt{(c_1-c_2)^2+(d_1-d_2)^2}\sqrt{((a_1-a_3)^2+(b_1-b_3)^2)((a_1-a_2)^2+(b_1-b_2)^2)-(a_1^2-a_1a_2+a_2a_3-a_3a_1+b_1^2-b_1b_2+b_2b_3-b_3b_1)^2}}$$

$$l_1 = \frac{(c_1^2-c_1c_2+c_2c_3-c_3c_1+d_1^2-d_1d_2+d_2d_3-d_3d_1)\sqrt{(a_1-a_2)^2+(b_1-b_2)^2}}{(a_1^2-a_1a_2+a_2a_3-a_3a_1+b_1^2-b_1b_2+b_2b_3-b_3b_1)\sqrt{(c_1-c_2)^2+(d_1-d_2)^2}}$$

$$\theta_1 = \frac{(a_1^2-a_1a_2+a_2a_3-a_3a_1+b_1^2-b_1b_2+b_2b_3-b_3b_1)}{\sqrt{((a_1-a_3)^2+(b_1-b_3)^2)((a_1-a_2)^2+(b_1-b_2)^2)-(a_1^2-a_1a_2+a_2a_3-a_3a_1+b_1^2-b_1b_2+b_2b_3-b_3b_1)^2}}$$

$$k_2 = \frac{\sqrt{(c_3-c_4)^2+(d_3-d_4)^2}}{\sqrt{(a_3-a_4)^2+(b_3-b_4)^2}}$$

$$m_2 = \frac{\sqrt{((c_3-c_1)^2+(d_3-d_1)^2)((c_3-c_4)^2+(d_3-d_4)^2)-(c_3^2-c_3c_4+c_4c_1-c_1c_3+d_3^2-d_3d_4+d_4d_1-d_1d_3)^2}\sqrt{(a_3-a_4)^2+(b_3-b_4)^2}}{\sqrt{(c_3-c_4)^2+(d_3-d_4)^2}\sqrt{((a_3-a_1)^2+(b_3-b_1)^2)((a_3-a_4)^2+(b_3-b_4)^2)-(a_3^2-a_3a_4+a_4a_1-a_1a_3+b_3^2-b_3b_4+b_4b_1-b_1b_3)^2}}$$

$$l_2 = \frac{(c_3^2-c_3c_4+c_4c_1-c_1c_3+d_3^2-d_3d_4+d_4d_1-d_1d_3)\sqrt{(a_3-a_4)^2+(b_3-b_4)^2}}{(a_3^2-a_3a_4+a_4a_1-a_1a_3+b_3^2-b_3b_4+b_4b_1-b_1b_3)\sqrt{(c_3-c_4)^2+(d_3-d_4)^2}}$$

$$\theta_2 = \frac{(a_3^2-a_3a_4+a_4a_1-a_1a_3+b_3^2-b_3b_4+b_4b_1-b_1b_3)}{\sqrt{((a_3-a_1)^2+(b_3-b_1)^2)((a_3-a_4)^2+(b_3-b_4)^2)-(a_3^2-a_3a_4+a_4a_1-a_1a_3+b_3^2-b_3b_4+b_4b_1-b_1b_3)^2}}.$$

REFERENCES

[1] L. L. Cristea and B. Steinsky, *Curves of infinite length in* 4×4 *labyrinth fractals*, Geom. Dedicata **141**, 2009, 1-17.
[2] L. L. Cristea and B. Steinsky, *Curves of infinite length in labyrinth fractals*, Proc. Edinb. Math. Soc. Ser.L.L. **54**(2), 2011 329-344.
[3] L.L. Cristea and Paul Surer, *Triangular labyrinth fractals*, Fractals, **27**(8), 2019, 1950131.
[4] L. L. Cristea and B. Steinsky, *Mixed labyrinth fractals,* Topology Appl.**229**, 2017, 112-125.
[5] L. L. Cristea and G. Leobacher, *Super-mixed labyrinth fractals*, J. Fractal Geom., 2018,
[6] A. A. Potapov, V. A. German and V. I. Grachev, *Nano and radar signal processing: Fractal reconstruction complicated images, signals and radar backgrounds based on fractal labyrinths*, 14th Int. Radar Symp. (I.R.S.), Dresden, Germany, 941-946, ISSN: 2155-5745.
[7] A. A. Potapov, V. A. German and V. I. Grachev, *Fractal labyrinths as a basis for reconstructing planar nanostructures*, Int. Conf. Electromagnetics in Advanced Applications (ICEAA), Turin, Italy, 2013, 949-952
[8] A. A. Potapov and W. Zhang, *Simulation of new ultra-wideband fractal antennas based on fractal labyrinths*, C.I.E. Int. Conf. Radar (RADAR), China, Guangzhou, 2016, 1-5.
[9] A. Potapov and V. Potapov, *Fractal radioelements, devices and systems for radar and future telecommunications: Antennas, capacitor, memristor, smart 2d frequency-selective surfaces, labyrinths and other fractal metamaterials*, J. Int. Sci. Publ. Mater. Methods Technol., **11**,2017, 492-512.
[10] D. Çelik, Y. Özdemir and M. Üreyen, *Affine contractions on the plane*, International Journal of Mathematical Education in Science and Technology, **38**(5),2007, 701-707.
[11] R. D. Mauldin and S. C. Williams, *Hausdorff dimension in graph directed constructions*, Trans. Am. Math. Soc., **309**, 1988, 811-829.
[12] J.R. Munkres,*Topology*, Prentice Hall, Inc., Second edition, 1975.

Harsha Gopalakrishnan is a research scholar in the Department of Mathematics and Statistics at the Indian Institute of Technology Tirupati. She completed her B.Sc in Mathematics from Kannur University in 2017 and her M.Sc in Mathematics from Calicut University in 2019. She qualified for CSIR-NET In 2019 and GATE in 2020 and 2021. Her research interests are Labyrinth Fractals and Analysis of Fractals.

Srijanani Anurag Prasad is an Assistant Professor in the Department of Mathematics and Statistics at the Indian Institute of Technology Tirupati (IITT). Prior to joining IITT, she was an Assistant Professor in the Department of Applied Science (Mathematics) at The North Cap University (N.C.U.) from Jan. 2016 to June 2017 and a Visiting Faculty at the Indian Institute of Science Education and Research Bhopal (IISERB) from July 2014 to Dec. 2015. Her research interests are Fractals, Fractal Interpolation Functions, Fractal Measure Theory, Labyrinth Fractals, Wavelets and Approximation.